Evidence for Interfacial-Storage Anomaly in Nanocomposites for Lithium Batteries from First-Principles Simulations

Yuri F. Zhukovskii,[1,2] Palani Balaya,[1] Eugene A. Kotomin,[1,2,*] and Joachim Maier[1]

[1]*Max-Planck-Institut für Festkörperforschung, Heisenbergstr.1, D-70569 Stuttgart, Germany*

[2]*Institute for Solid State Physics, University of Latvia, Kengaraga 8, LV- 1063 Riga, Latvia*

(Received 12 October 2005; published 9 February 2006)

We present theoretical support for a mass storage anomaly proposed for nanocomposites in the context of lithium batteries which forms the transition between an electrostatic capacitive mechanism and an electrode mechanism. *Ab initio* atomic and electronic structure calculations, performed on the Ti(0001)/Li_2O(111) model interface, indicate the validity of the phenomenological model of interfacial Li storage and provide a deeper insight into the local situation. Beyond the specific applicability to storage devices, the possibility of a two-phase effect on mass storage generally highlights the availability of novel degrees of freedom in materials research when dealing with nanocomposites.

DOI: 10.1103/PhysRevLett.96.058302 PACS numbers: 82.47.Aa, 71.15.−m, 73.40.Ns, 82.45.Yz

In nanostructured solids, interfacial effects can play a dominant role due to the substantial proportion of the interfaces but even more noticeably because of their finite spacing leading to size effects [1–3]. As this refers to local composition and charge distribution, not only transport properties but also mass storage phenomena are affected. As far as electrical storage devices are concerned, one has to distinguish between electrostatic capacitors where charges are accommodated at surfaces and batteries where the charge storage occurs electrochemically in the bulk of electrodes. Whilst in the latter case the capacity is much higher, the former devices have advantage in terms of the rate performance. Li batteries present the most important electrochemical storage devices since most of today's high-performance portable microelectronic devices demand high energy densities. A recent striking observation in Me/Li_2O nanocomposites (where Me means transition metals such as Co, Cu, Fe, Ni, etc. that do not alloy with Li), investigated for rechargeable Li batteries, is the occurrence of an extra Li storage at low potential [4]. An interfacial charge storage mechanism was proposed recently to explain the origin for this anomaly [5]. According to this model, Li^+ ions are stored on the oxide's side of the interface while electrons (e^-) are localized on the metallic side resulting in a charge separation. If the spacing of the interface is of the order of the screening length the difference between a capacitor and a battery is blurred. The mechanism can be generalized to a storage of a compound A^+B^- at the interface of two phases, α and β, whereby only A^+ can be stored in α and only B^- can be stored in β (see Fig. 1).

In this Letter, we present results of *ab initio* calculations along with recent experimental results to support this interfacial-storage mechanism. *Ab initio* simulations can reliably describe the electronic structure of various Me/Li_2O interfaces, which play a crucial role in the proper interpretation of experimentally observed phenomena at the microscopic level. As in our case, unambiguous experimental evidence is difficult to achieve for the interfacial-storage mechanism; the simulation approach could be particularly helpful. Complementation of experimental results in the field of Li batteries by *ab initio* modeling was also found to be very fruitful in investigating the electronic and electrochemical properties of titania [6].

Let us briefly describe the experimental facts of our Li battery example and concentrate on RuO_2 which is taken as a model electrode material in this context. Incorporation of 4Li per RuO_2 formula unit leads to the formation of a Ru/Li_2O nanocomposite with crystallite sizes of 2–5 nm [7]. Further incorporation (up to 5.6Li per RuO_2) results in a sloped behavior. On charging, if the voltage is limited between 0.02–1.2 V (as the slope ends at 1.2 V), a reversible Li-storage capacity of 120 mA h/g is observed at a slow rate (i.e., discharge in 45 min) with a capacitive behavior as shown in Fig. 2. A storage capacity of 70 mA h/g was achieved at a fast rate (i.e., discharge in 1.3 min) within this voltage window. A similar behavior observed in the Co/Li_2O nanocomposite at low potential has been tentatively explained by a reaction of Li with the conducting-type polymeric film formed *in situ* [4].

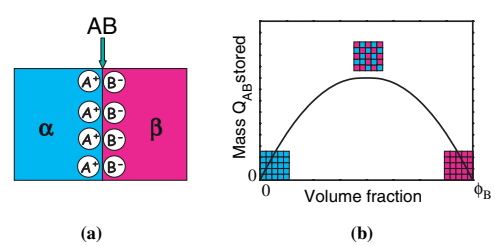

FIG. 1 (color). (a) Phenomenological model for the explanation of extra mass storage due to the interfacial-storage mechanism [5]. (b) Schematic representation mass storage (A^+B^-) in a nanocomposite α-β whereby AB is insoluble in both α and β. The solubility in α/α and β/β grain boundaries is neglected. In both cases, α refers to Li_2O and β refers to an inert metal while A^+ and B^- are Li^+ and e^-, respectively.

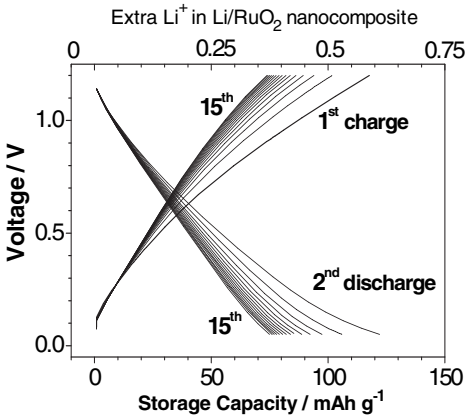

FIG. 2. Electrochemical charge-discharge curve of RuO_2/Li cell between the voltage window 0.02–1.2 V.

However, at least in the case of Ru/Li_2O nanocomposite, it is clear from the high resolution transmission electron microscope images [7] that the passivation layer mainly decomposes on charge beyond the sloped region (1.2 V). This observation and the fact that the storage can occur even at a fast rate suggest that the extra Li storage is due to a process that is different from the homogeneous insertion and heterogeneous conversion reactions. Another explanation can be the segregation of metal at the grain boundaries/interface and subsequent alloy reaction of metal with the incorporated Li [8]. This possibility is, however, ruled out in the case of the Ru/Li_2O nanocomposite, as no alloy reaction is known between Ru and Li metals.

To perform the first-principles simulation of the extra Li storage using a model of the defect-free Me/Li_2O interface, we have considered a two-dimensional slab containing several layers of metal and oxide. The antifluorite cubic structure of Li_2O single crystal is described by $Fm3m$ space group (lattice constant $a_0 = 4.61$ Å), whereas the hexagonal hcp structure of Co, Ru, and Ti belongs to a $P63/mmc$ space group (for the latter, $a_0 = 2.95$ Å, $c_0 = 4.68$ Å) [9]. Lattice mismatch between the symmetrically compatible $Li_2O(111)$ and Ti(0001) surfaces is markedly smaller (~9%) than for the interfaces between the same lithia substrate and either Ru(0001) or Co(0001) surface (~18% and ~24%, respectively). Thus, the perfect $Ti(0001)/Li_2O(111)$ interface should be structurally more stable than both $Ru(0001)/Li_2O(111)$ and $Co(0001)/Li_2O(111)$ interfaces. This is why—although Li incorporation into TiO_2 cannot reduce this to metal—$Ti/Li_2O(111)$ has been chosen in the present study as a model interface, in order to describe experimentally studied Me/Li_2O nanocomposites. To simulate the $Ti(0001)/Li_2O(111)$ interface, we have performed *ab initio* density functional theory (DFT) calculations using the hybrid B3PW method, which includes a partial incorporation of the exact Hartree-Fock (HF) nonlocal exchange into the DFT exchange functional, with a varying mixing ratio [as implemented in CRYSTAL-03 code [10]]. Both DFT and HF methods are realized in this code in the framework of the Gaussian-type functions (GTFs) formalism. The all-valence basis sets for Li, O, and Ti GTFs had been optimized elsewhere [for Li_2O single crystal [11] and for some Ti-containing crystalline compounds [12]].

Here we mainly analyze the calculated parameters of electronic charge redistribution and total energy for three different configurations of defect-free $Ti/Li_2O(111)$ interface (Tables I and II). For this purpose, we have calculated slab models containing 5–7 (111) planes of Li_2O (single crystal) in contact with one (two) Ti(0001) planes. To vary the Li atom concentration on the Ti/Li_2O interface between the O-terminated substrate and Ti adlayer from zero up to 2.25 monolayer (ML) as shown in Table I, we have considered 2×2 surface supercells. Extra Li atoms have been placed in several positions, including both sides of the $Li_2O(111)$ slabs: (i) above the outermost Li (or O) plane under the Ti adlayer, (ii) on the opposite side of the slab which does not contain adsorbed Ti layer, (iii) in several sites inside the slab. For each interfacial configuration containing Li extra atoms, we have performed geometry optimization for the first coordination sphere of atoms around the impurity and the closest interlayer distances. The total geometry optimization of these systems is extremely time consuming; this is why relative energies for extra Li positions inside a slab are overestimated in our calculations (Table I). This is, however, not so important for a qualitative description of the interfacial Li-storage mechanism. As a result, we have found several energetically favorable positions for the extra Li atoms. A comparison of the calculated relative energies for all configurations of the $Ti/Li_2O(111)$ interface presented in Table I shows that extra Li atoms prefer to be localized at the Li_2O surface as well as at the Ti/Li_2O interface rather than inside the slab. It is worth mentioning that unlike the free surface, the Ti/Li_2O interface is the relevant one if comparison with the experiment is made.

Let us first consider the O-terminated Ti/Li_2O interface shown in part (a) of Table I (called hereafter *understoichiometric* $Li_{2-\delta}O$ substrate, $\delta > 0$). Obviously, both extra Li atoms and Ti adatoms donate electronic charge towards the outermost oxygen ions, which are still undersaturated in terms of the electron density and hence are strongly oxidizing. At the Li-terminated Ti/Li_2O interface corresponding to *stoichiometric* Li_2O [i.e., $\delta = 0$, part (b) of Table I], extra Li atoms, in line with the chemical expectations, begin to donate their electronic charge towards Ti adatoms while the interface oxygen ions tend to achieve the full effective charge $-2e$. For a furthermore enhanced lithium density in the $Ti/Li_2O(111)$ interface [*overstoichiometric* $Li_{2+\delta}O$ substrate, part (c) of Table I], the electronic charge induced on Ti adatoms rapidly increases, whereas ionicity of the interfacial Li slightly decreases. It is noteworthy how the character of electron transfer between Ti and $Li_{2\pm\delta}O$ changes from an electron donor to an electron acceptor (Table II), namely, from $+0.84$ up to $-0.54e$ (or even $-0.75e$ when a second layer of Ti is added—not listed

TABLE I. Charge and energy parameters for different configurations of Ti/Li_2O interface. Extra Li—effective charge on extra lithium atom, O-av. and Ti-av.—average effective charge on O-and Ti-layer *per* atom.

Reaction step	Relative energy (eV)	Induced charge for different configurations (e) Extra Li	O-av	Ti-av	Graphic images of interfacial cross sections
	(a)	"*Understoichiometric*"		O-terminated	interface
(a) Extra Li atom positioned on the plane of $Li_2O(111)$ slab opposite to the interface	**0**	0.94	−1.94	0.84	
(b) Extra Li atom between the deep internal lithium layers	**3.86**	0.88	−1.91	0.75	
(c) Extra Li atom between the O-terminated substrate and titanium adlayer	**1.05**	0.917	−1.80	0.55	
	(b)	*Stoichiometric*		Li-terminated	interface
(a) Extra Li atom positioned on the plane of $Li_2O(111)$ slab opposite to the Ti/Li_2O interface	**0**	0.96	−2.0	0.21	
(b) Extra Li atom between the deep internal Li layers	**8.20**	0.84	−2.0	0.18	
(c) Extra Li atom over the outermost O layer	**4.76**	0.92	−1.9	−0.16	
(d) Extra Li atom over the outermost interfacial Li layer	**0.77**	0.79	−2.0	−0.12	
	(c)	"*Overstoichiometric*"		Li-terminated	interface
(a) Extra Li atom positioned above the plane of $Li_2O(111)$ slab opposite to the Ti/Li_2O interface	**0**	0.92	−2.0	−0.47	
(b) Extra Li atom at the middle level of the interfacial Li double layer under titanium monolayer	**1.34**	0.78	−2.0	−0.54	
(c) Extra Li atom positioned above the outermost Li double layer under titanium monolayer	**1.87**	0.44	−2.0	−0.46	

in Table II). To illustrate the influence of extra Li atoms on the electronic charge transfer in the $Ti/Li_2O(111)$ interface, let us consider Fig. 3 which shows the electronic charge redistributions for concentrations of Li atoms between the Ti adlayer and outermost O layer being 1 ML [Fig. 3(a)] and 1.25 ML [Fig. 3(b)]. Parameters of induced electronic charges for these configurations are presented in Table II. It is clearly seen that the extra Li atom causes an additional electronic charge transfer towards the Ti adlayer. Moreover, redistribution of the electronic charge around the extra Li atom [Fig. 3(b)] is evidently nonhomogeneous: in the close vicinity of Li, the Ti adatom still transfers its charge towards the substrate surface whereas three other Ti adatoms accept substantially larger electronic densities which results in the transfer of average electronic charge towards adlayer $\sim 0.12e$ (Table II), i.e., by $0.3e$ larger than without extra Li atom [Fig. 3(a)].

The affinity of the Li atom while bringing it from infinity towards the interface of $Ti/Li_2O(111)$ composite depends on the detailed composition. The corresponding values are 7.2, 5.3, and 3.9 eV for the *understoichiometric*, *stoichiometric*, and *overstoichiometric* interfaces, respectively. The larger the density of interfacial lithium, the closer the affinity of Li atoms towards the Li_2O surface compared

TABLE II. Dependence of the interfacial charge transfer on the concentration of Li atoms between the Ti adlayer and outermost O layer (see Table I for description of symbols).

O-terminated interface														
0 ML			1/4 ML			1/2 ML			3/4 ML			4/4 ML		
Extra Li	O-av.	Ti-av.	Extra Li	O-av.	Ti-av.	Extra Li	O-av.	Ti-av.	Extra Li	O-av.	Ti-av.	Extra Li	O-av.	Ti-av.
···	−1.94	0.84	0.92	−1.8	0.55	0.91	−1.86	0.39	0.90	−1.92	0.29	0.89	−2.0	0.18
Li-terminated interface														
5/4 ML			6/4 ML			7/4 ML			8/4(2) ML			9/4 ML		
Extra Li	O-av.	Ti-av.	Extra Li	O-av.	Ti-av.	Extra Li	O-av.	Ti-av.	Extra Li	O-av.	Ti-av.	Extra Li	O-av.	Ti-av.
0.81	−2.0	−0.12	0.79	−2.0	−0.23	0.77	−2.0	−0.34	0.73	−2.0	−0.46	0.78	−2.0	−0.54

to the aforementioned cohesion energy of Li bulk [1.7 eV [13]]. This means that the localization of an extra Li atom at even the overstoichiometric interface is still more favorable energetically than residing within Li bulk metal [the reader may note that the affinity (3.9 eV–1.7 eV ≈ 2.2 eV) even in the overstoichiometric case is larger than experimental values (Co, Ru, etc. ≤ 1 eV); in how far this is due to a model used in our calculations will be considered in a forthcoming paper]. In terms of charge transfer, our model is similar to that of nonstoichiometric Mg-terminated (111) surface of MgO [14]. Clearly, when we compare the storage of a Ti/Li_2O nanocomposite with an equivalent Ti or Li_2O massive crystal (see Fig. 1), the present calculations indicate a substantial excess storage at the Ti/Li_2O interface. However, we cannot extract from them, in how far grain boundaries in nanocrystalline Ti or Li_2O can also store Li (neglected in Fig. 1).

In summary, several important conclusions can be drawn. The extra capacity, obtained in metal/Li_2O nanocomposite, can be explained by an interfacial-storage mechanism [5]. Compared to pure Li_2O or Ti bulk, a Ti/Li_2O (saturated with Li) interface can store at least a monolayer of additional Li per interface with electrons being transferred largely to the titanium adatoms, in full accordance with this mechanism. It has been found that a free (stoichiometric) Li_2O slab can also store excess surface Li mostly distributed within the Li_2O (i.e., lowering the average Li^+ charge). Note, however, that the free Li_2O surfaces are high energy surfaces. While Li_2O surface layers or the interfacial core serve as hosts for Li^+, the Ti serves as an electron sink, a role which is more pronounced, the thicker the slab owing to the stabilization of the electron. The effect is also expected to increase if Ti is replaced by another metal (e.g., Ru). When making Li_2O progressively understoichiometric by removing Li, the role of Ti changes from an electron acceptor to an electron donor, in agreement with the chemical expectations. In more general terms, present study shows that a storage anomaly described in Fig. 1 is possible and that the stoichiometry of small systems and nanocomposites can be significantly different from the bulk phases. For the specific case of energy research this phenomenon describes the bridge between a capacitor and an electrode behavior referring to a situation in which an optimization of storage capacity versus storage rate should be possible.

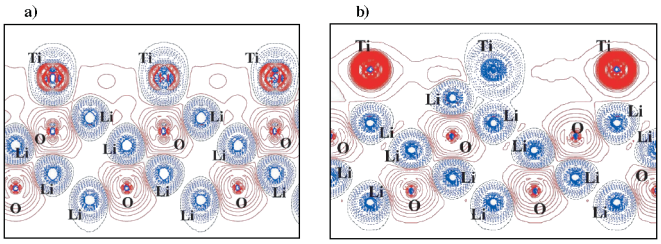

FIG. 3 (color). 2D difference electron density maps $\Delta\rho(\mathbf{r})$ in the cross section perpendicular to the interface plane are shown for two different atomic fractions of lithium in the $Ti/Li_2O(111)$ interface: 1 ML (a) and 1.25 ML (b). Isodensity curves are drawn from $-0.2e$ Å^{-3} to $+0.2e$ Å^{-3} with an increment $0.002e$ Å^{-3}. The full (red) and dashed (blue) curves show positive and negative difference electron densities, respectively.

The authors thank E. U. for support through the ALISTORE project and J. Jamnik for useful discussion.

*Email address: s.weiglein@fkf.mpg.de

[1] J. Maier, Prog. Solid St. Chem. **23**, 171 (1995); Nat. Mater. **4**, 805 (2005).
[2] H. L. Tuller, Solid State Ionics **131**, 143 (2000).
[3] J. Schoonman, Solid State Ionics **135**, 5 (2000).
[4] P. Poizot *et al.*, Nature (London) **407**, 496 (2000); S. Laruelle *et al.*, J. Electrochem. Soc. **149**, A627 (2002).
[5] J. Jamnik and J. Maier, Phys. Chem. Chem. Phys. **5**, 5215 (2003).
[6] M. V. Koudriachova, S. W. de Leeuw, and N. M. Harrison, Phys. Rev. B **69**, 054106 (2004).
[7] P. Balaya *et al.*, Adv. Funct. Mater. **13**, 621 (2003).
[8] L. Y. Beaulieu *et al.*, J. Electrochem. Soc. **147**, 3206 (2000).
[9] R. W. G. Wyckoff, *Crystal Structures* (Wiley, New York, 1963), Vol. 1.
[10] V. R. Saunders *et al.*, *CRYSTAL-03 User Manual* (University of Turin, Italy, 2003).
[11] R. Dovesi *et al.*, Chem. Phys. **156**, 11 (1991).
[12] C. M. Zicovich-Wilson and R. Dovesi, J. Phys. Chem. B **102**, 1411 (1998).
[13] R. E. McLaren and C. A. Sholl, J. Phys. F **4**, 2172 (1974).
[14] A. Subramanian *et al.*, Phys. Rev. Lett. **92**, 026101 (2004).